processes

Article

Network Pharmacology Study to Interpret Signaling Pathways of *Ilex cornuta* Leaves against Obesity

Ki-Kwang Oh [ID]**, Md. Adnan** [ID] **and Dong-Ha Cho** *

Department of Bio-Health Convergence, College of Biomedical Science, Kangwon National University, Chuncheon 24341, Korea; nivirna07@kangwon.ac.kr (K.-K.O.); mdadnan1991.pharma@gmail.com (M.A.)
* Correspondence: chodh@kangwon.ac.kr; Tel.: +82-33-250-6475; Fax: +82-33-259-5642

Abstract: *Ilex cornuta* Leaves (ICLs) are a representative and traditional prescription for controlling obesity. Nevertheless, the corresponding therapeutic compounds and related pharmacological mechanisms of such medication remain undocumented. The compounds from ICLs were identified by gas chromatography-mass spectrum (GC-MS), and SwissADME confirmed their physicochemical properties. Next, the target proteins related to compounds or obesity-associated proteins were retrieved from public databases. RPackage constructed the protein–protein interaction (PPI) network, a bubble chart, and signaling pathways–target proteins–compounds (STC) network. Lastly, a molecular docking test (MDT) was performed to evaluate the affinity between target proteins and ligands from ICLs. GC-MS detected a total of 51 compounds from ICLs. The public databases identified 219 target proteins associated with selective compounds, 3028 obesity-related target proteins, and 118 overlapping target proteins. Moreover, the STC network revealed 42 target proteins, 22 signaling pathways, and 39 compounds, which were viewed to be remedially significant. The NOD-like receptor (NLR) signaling pathway was considered a key signaling pathway from the bubble chart. In parallel, the MDT identified three target proteins (IL6, MAPK1, and CASP1) on the NLR signaling pathway and four compounds against obesity. Overall, four compounds from ICLs might show anti-obesity synergistic efficacy by inactivating the NLR signaling pathway.

Keywords: *Ilex cornuta* Leaves; obesity; network pharmacology; NOD-like receptor signaling pathway

1. Introduction

Obesity has now sharply hit epidemic levels and has become a significant cause of global death [1]. A recent report indicates that obesity is closely linked to metabolic disorders that distinctly develop psychological stress and often exacerbate obesity-related complications [2]. Obesity can present in all ages; in 2016, almost 13% of the world population were overweight [3]. Moreover, obesity is deeply associated with other metabolic diseases such as diabetes, hypertension, atherosclerosis, and heart failure [4]. The main driving factors of metabolic disorders are cytokines, which are mainly implicated with a high-fat diet [5]. Currently, available anti-obesity medications include sibutramine, rimonabant, and orlistat, which may lead to side effects like diarrhea, fecal incontinence, flatulence, and dyspepsia [6,7]. In contrast, herbal solutions based on natural organic compounds have been used for thousands of years with high efficacy and safety [8]. To date, many natural herbal plants are used in a diet regime or as an alleviator for anti-obesity [9], for example, *Ilex cornuta* Leaves (ICLs) are potentially used to treat obesity. A topical patent on ICLs summarized that the extract could be effective for various metabolic diseases [10]. Moreover, some reports demonstrated that ICLs extract has potent anti-inflammatory effects associated with obesity in adipocytes [11,12]. Another study stated that the *Ilex* species, including ICLs, are known for regulating lipid metabolism and weight-loss activity [13]. Until now, research of ICLs has been focused on a broad range of metabolic disorders without defining the exact action mechanism for particular diseases. Therefore,

the studies on active compounds and mechanisms of ICLs against obesity should be proven to understand the pharmacological value in alleviating obesity.

Network pharmacology is an efficient method to comprehend relationships between multiple unspecific compounds and multiple target proteins [14]. It is a relatively effective technique to analyze herbal medicines regarding novel active compounds and new mechanisms of action against different diseases [15]. Mainly, for metabolic syndrome research, the network pharmacology approach contributes to unravelling complex biological systems and interactions between active compounds and target proteins [16,17].

The concept and principle of network pharmacology proposed by Andrew Hopkins are based on bioinformatics and system biology [18]. In addition, the development of bioinformatics with system biology supports the progression of network pharmacology; for instance, Dr. Shoichet's group expanded the 'similarity ensemble approach' to search the connectivity between ligand and target protein [19]. SwissTargetPrediction (STP) is a web-based bioinformatics database developed by the SIB (Swiss Institute of Bioinformatics), which loaded 376,342 reliable experimental compounds and 3,068 target proteins since 2014 [20]. Likewise, Dr. Furlong developed 'DisGeNET', a comprehensive platform for the efficient exploration of 380,000 associations between 13,000 diseases and more than 16,000 genes [21]. Furthermore, Online Mendelian Inheritance in Man (OMIM) is integrated with other genetic databases such as PubMed references, DNA and protein sequence, and the specific mutation database [22]. Thus, this study utilized these four databases to understand the relationships between compounds from ICLs and obesity-related target proteins from a human. To sum things up, network pharmacology utilized via four bioinformatics explored the mechanisms of ICLs against obesity and found promising active compounds from ICLs and associated target proteins. The functional diagram is exhibited in Figure 1.

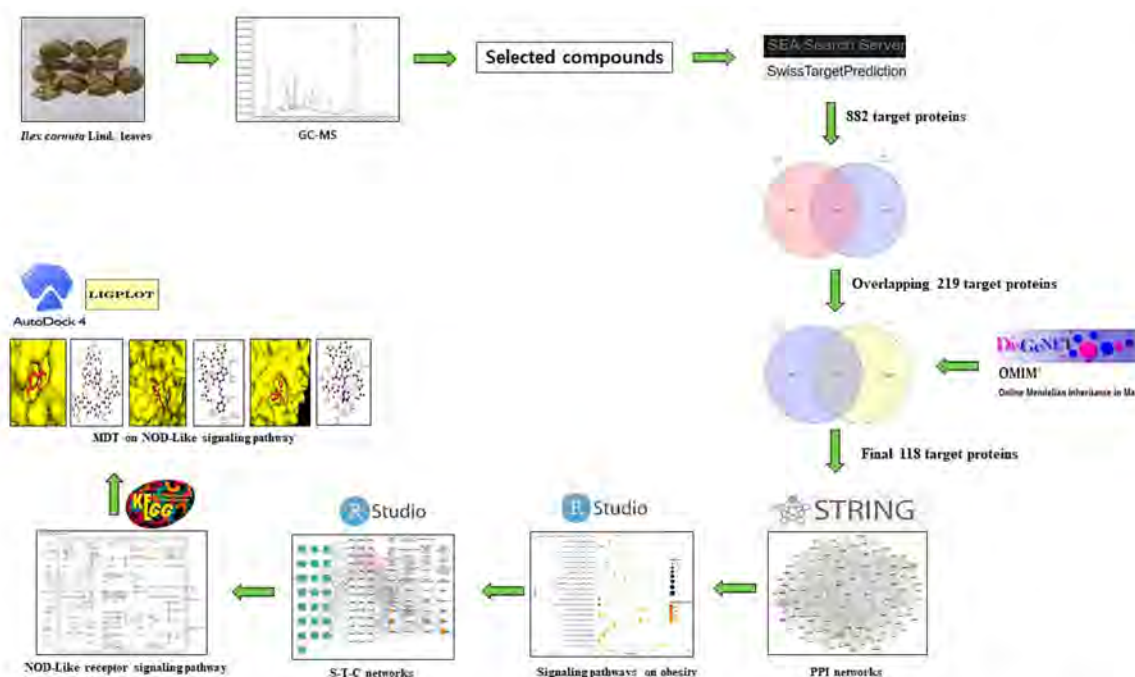**Figure 1.** Workflow diagram of network pharmacology analysis of ICLs against obesity.

2. Results

2.1. Chemical Compounds from ICLs

A total of 52 chemical compounds in ICLs were identified by the GC-MS analysis (Figure 2), and the name of compounds, PubChem ID, retention time (min), peak area (%), and pharmacological activities were enlisted in Table 1. Lipinski's rules accepted the

number of 51 out of 52 chemical compounds (molecular weight ≤ 500g/mol; Moriguchi octanol-water partition coefficient ≤4.15; number of nitrogen or oxygen ≤10; number of NH or OH ≤5), and the selected 51 chemical compounds (excluding lactose) corresponded with the standard of 'Abbott Bioavailability Score (>0.1)' through SwissADME. Additionally, lactose was excluded due to the number of nitrogen or oxygen and the number of NH or OH. The TPSA (topological polar surface area) value of the selected 51 chemical compounds (excluding lactose) was also accepted (Table 2).
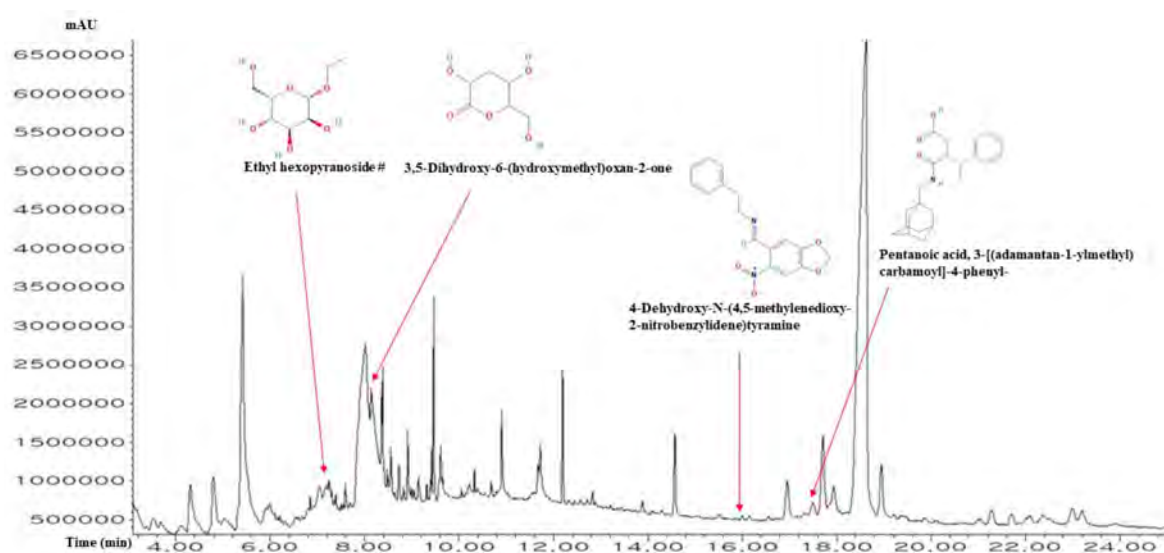

Figure 2. A typical GC-MS peak of ICLs.

Table 1. A list of 52 chemical compounds identified from ICLs via GC-MS and profiling of biological activities.

No.	Compounds	Pubchem ID	RT (mins)	Area (%)	Pharmacological Activities (Reference)
1	N-Acetylmannosamine	11,096,158	3.520	0.49	No reports
2	1-Aminopropan-2-ol	4	3.683	0.41	Anti-malaria [23]
3	2-Propenethioamide, 3-(acetyloxy)-N,N-dimethyl-, (E)-	5,363,184	4.135	0.46	No reports
4	2-Hydroxy-3-methyl-4H-pyran-4-one	54,681,620	4.318	2.34	No reports
5	4H-Pyran-4-one, 2,3-dihydro-3,5-dihydroxy-6-methyl-	119,838	4.799	1.98	No reports
6	Tetrahydrofuran-3,4-diol	90,803	5.039	0.84	No reports
7	5-Hydroxymethylfurfural	237,332	5.424	9.54	No reports
8	Ascaridole	10,545	5.943	0.34	Anti-neoplasms (PCIDB)
9	1-Nonene	31,285	6.000	0.30	No reports
10	Fumaramic acid	5,364,140	6.539	0.22	No reports
11	2,1,3-Benzothiadiazole	67,502	6.808	0.43	No reports
12	Hypoxanthine	135,398,638	6.856	0.32	Anti-gout (PCIDB)
13	Guanidine, 1-ethyl-3-nitro-	135,515,028	7.049	1.79	No reports
14	Levoglucosan	2,724,705	7.202	1.18	No reports
15	Ethyl-α-d-glucopyranoside	91,694,274	7.250	0.82	No reports
16	2-(4-Methylcyclohexyl)prop-2-en-1-ol	543,946	7.606	0.45	No reports
17	Octanoic acid	379	8.020	12.91	Antimicrobial [24]

Table 1. *Cont*.

No.	Compounds	Pubchem ID	RT (mins)	Area (%)	Pharmacological Activities (Reference)
18	3,5-Dihydroxy-6-(hydroxymethyl)oxan-2-one	541,561	8.145	5.95	No reports
19	2-Isopropenylthiophene	121,729	8.385	2.82	No reports
20	Sulfallate	7216	8.481	0.55	No reports
21	Crocetane	136,331	8.568	0.94	No reports
22	Diphenylmethane	7580	8.731	0.67	No reports
23	Palmitic acid	985	8.914	0.87	Anti-cancer
24	1-(3-Butyn-2-yloxy)-1-methyl-1-silacyclohexane	597,458	9.154	0.47	No reports
25	Lactose	6134	9.318	0.20	Thyroid cancer(marker) (PCIDB)
26	Methyl linoleate	5,284,421	9.424	0.45	No reports
27	Phytol	5,366,244	9.462	1.28	Anti-necrosis (PCIDB)
28	cis,cis,cis-7,10,13-Hexadecatrienal	5,367,366	9.616	0.82	No reports
29	Linolenic acid	5,280,934	9.654	0.32	Anti-inflammation [23]
30	Phytone	10,408	10.058	0.06	No reports
31	11-Dodecynyl acetate	538,082	10.222	0.43	No reports
32	1-(Pyrrolidinocarbonylmethyl)piperazine	100,614	10.327	0.26	No reports
33	Amonafide	50,515	10.693	0.14	No reports
34	2-Palmitoylglycerol	123,409	10.904	1.02	No reports
35	7-Pentadecyne	549,063	11.683	0.49	No reports
36	cis,cis,cis-7,10,13-Hexadecatrienal	5,367,366	11.722	1.41	No reports
37	Squalene	638,072	12.202	1.24	Anti-leukemia
38	2-Methyl-3-(3-methyl-but-2-enyl)-2-(4-methyl-pent-3-enyl)-oxetane	550,119	12.827	0.23	No reports
39	Stigmastan-3-ol	6743	13.895	0.24	No reports
40	Vitamin E	14,985	14.577	1.28	Anti-oxidant [23]
41	4-Cyclohexene-1,2-dicarboximide, N-butyl-, cis-	91,733,922	15.520	0.10	No reports
42	4-Dehydroxy-N-(4,5-methylenedioxy-2-nitrobenzylidene)tyramine	610,062	16.000	0.08	No reports
43	Clionasterol	457,801	16.962	1.14	Anti-ischemic (PCIDB)
44	17-(1,5-Dimethylhexyl)-10,13-dimethyl-4-vinylhexadecahydrocyclopenta[a]phenanthren-3-ol	537,099	17.318	0.24	No reports
45	Pentanoic acid, 3-[(adamantan-1-ylmethyl)carbamoyl]-4-phenyl-	4,920,612	17.500	0.67	No reports
46	β-amyrenol	225,689	17.712	2.47	No reports
47	Ethyl 2-(2-chloroacetamido)-3,3,3-trifluoro-2-(3-fluoroanilino)propionate	610,054	17.933	1.71	No reports
48	Lupeol	259,846	18.625	31.17	Anti-carcinoma [25]
49	Ethyl 2-[(2-chloroacetyl)amino]-3,3,3-trifluoro-2-(4-fluoroanilino)propanoate	610,053	21.020	0.24	No reports
50	Lanosterol	246,983	21.289	0.53	Anti-osteosarcoma [26]
51	Cycloisolongifolene, 7-bromo-	608,988	21.712	0.37	No reports
52	Cycloeucalenyl acetate	537,081	23.202	0.64	No reports

PCIDB: Phyto Chemical Interactions DB (https://www.genome.jp/db/pcidb) (accessed on 28 April 2021).

Table 2. Physicochemical properties of chemical compounds for good oral bioavailability and cell membrane permeability.

No.	Compounds	Lipinski Rules				Lipinski's Violations	Bioavailability Score	TPSA (Å²)
		MW	HBA	HBD	MLog P			
		<500	<10	≤5	≤4.15	≤1	>0.1	<140
1	N-Acetylmannosamine	221.21	6	5	−2.61	0	0.55	119.25
2	1-Aminopropan-2-ol	75.11	2	2	−0.63	0	0.55	46.25
3	2-Propenethioamide, 3-(acetyloxy)-N,N-dimethyl-, (E)-	173.23	2	0	0.54	0	0.55	61.63
4	2-Hydroxy-3-methyl-4H-pyran-4-one	126.11	3	1	−0.03	0	0.55	50.44
5	4H-Pyran-4-one, 2,3-dihydro-3,5-dihydroxy-6-methyl-	144.13	4	2	−1.77	0	0.85	66.76
6	Tetrahydrofuran-3,4-diol	104.10	3	2	−1.45	0	0.55	49.69
7	5-Hydroxymethylfurfural	126.11	3	1	−1.06	0	0.55	50.44
8	Ascaridole	168.23	2	0	2.19	0	0.55	18.46
9	1-Nonene	126.24	0	0	4.38	1	0.55	0.00
10	Fumaramic acid	115.09	3	2	−1.04	0	0.56	80.39
11	2,1,3-Benzothiadiazole	136.17	2	0	0.63	0	0.55	54.02
12	Hypoxanthine	136.11	3	2	−1.17	0	0.55	74.43
13	Guanidine, 1-ethyl-3-nitro-	132.12	3	2	−0.94	0	0.55	96.23
14	Levoglucosan	162.14	5	3	−1.94	0	0.55	79.15
15	Ethyl-α-d-glucopyranoside	208.21	6	4	−2.07	0	0.55	99.38
16	2-(4-Methylcyclohexyl)prop-2-en-1-ol	154.25	1	1	2.30	0	0.55	20.23
17	Octanoic acid	144.21	2	1	1.96	0	0.85	37.30
18	3,5-Dihydroxy-6-(hydroxymethyl)oxan-2-one	162.14	5	3	−1.68	0	0.55	86.99
19	2-Isopropenylthiophene	124.20	0	0	2.17	0	0.55	28.24
20	Sulfallate	223.79	0	0	2.28	0	0.55	60.63
21	Crocetane	282.55	0	0	7.38	1	0.55	0.00
22	Diphenylmethane	168.23	0	0	5.06	1	0.55	0.00
23	Palmitic acid	256.42	2	1	4.19	1	0.85	37.30
24	1-(3-Butyn-2-yloxy)-1-methyl-1-silacyclohexane	182.33	1	0	2.30	0	0.55	9.23
25	Lactose	342.30	11	8	−4.37	2	0.17	189.53
26	Methyl linoleate	294.47	2	0	4.70	1	0.55	26.30
27	Phytol	296.53	1	1	5.25	1	0.55	20.23
28	cis,cis,cis-7,10,13-Hexadecatrienal	234.38	1	0	4.01	0	0.55	17.07
29	Linolenic acid	278.43	2	1	4.38	1	0.85	37.30
30	PHYTONE	268.48	1	0	4.79	1	0.55	17.07
31	11-Dodecynyl acetate	224.34	2	0	3.58	0	0.55	26.30
32	1-(Pyrrolidinocarbonylmethyl)piperazine	197.28	3	1	0.05	0	0.55	35.58
33	Amonafide	283.33	3	1	1.71	0	0.55	68.33
34	2-Palmitoylglycerol	330.50	4	2	3.18	0	0.55	66.76
35	7-Pentadecyne	208.38	0	0	6.04	1	0.55	0.00
36	cis,cis,cis-7,10,13-Hexadecatrienal	234.38	1	0	4.01	0	0.55	17.07
37	Squalene	410.72	0	0	7.93	1	0.55	0.00
38	2-Methyl-3-(3-methyl-but-2-enyl)-2-(4-methyl-pent-3-enyl)-oxetane	222.37	1	0	3.56	0	0.55	9.23
39	Stigmastan-3-ol	416.72	1	1	6.88	1	0.55	20.23
40	Vitamin E	430.71	2	1	6.14	1	0.55	29.46
41	4-Cyclohexene-1,2-dicarboximide, N-butyl-, cis-	207.27	2	0	1.68	0	0.55	37.38
42	4-Dehydroxy-N-(4,5-methylenedioxy-2-nitrobenzylidene)tyramine	298.29	5	0	1.49	0	0.55	76.64
43	Clionasterol	414.71	1	1	6.73	1	0.55	20.23
44	17-(1,5-Dimethylhexyl)-10,13-dimethyl-4-vinylhexadecahydrocyclopenta[a]phenanthren-3-ol	414.71	1	1	6.73	1	0.55	20.23
45	Pentanoic acid, 3-[(adamantan-1-ylmethyl)carbamoyl]-4-phenyl-	369.50	3	2	3.69	0	0.85	66.40
46	beta-Amyrenol	426.72	1	1	6.92	1	0.55	20.23
47	Ethyl 2-(2-chloroacetamido)-3,3,3-trifluoro-2-(3-fluoroanilino)propionate	356.70	7	2	2.60	0	0.55	67.43
48	Lupeol	426.72	1	1	6.92	1	0.55	20.23
49	Ethyl 2-[(2-chloroacetyl)amino]-3,3,3-trifluoro-2-(4-fluoroanilino)propanoate	356.70	7	2	2.60	0	0.55	67.43
50	Lanosterol	426.72	1	1	6.82	1	0.55	20.23
51	Cycloisolongifolene, 7-bromo-	283.25	0	0	5.26	1	0.55	0.00
52	Cycloeucalenyl acetate	468.75	2	0	7.08	1	0.55	26.30

2.2. Overlapping Target Proteins between SEA and STP

A total of 525 target proteins from SEA and 576 target proteins from STP connected to 51 chemical compounds were identified (Supplementary Table S1). The Venn diagram showed that 219 target proteins were overlapped between the two compound databases (Supplementary Table S1) (Figure 3A).
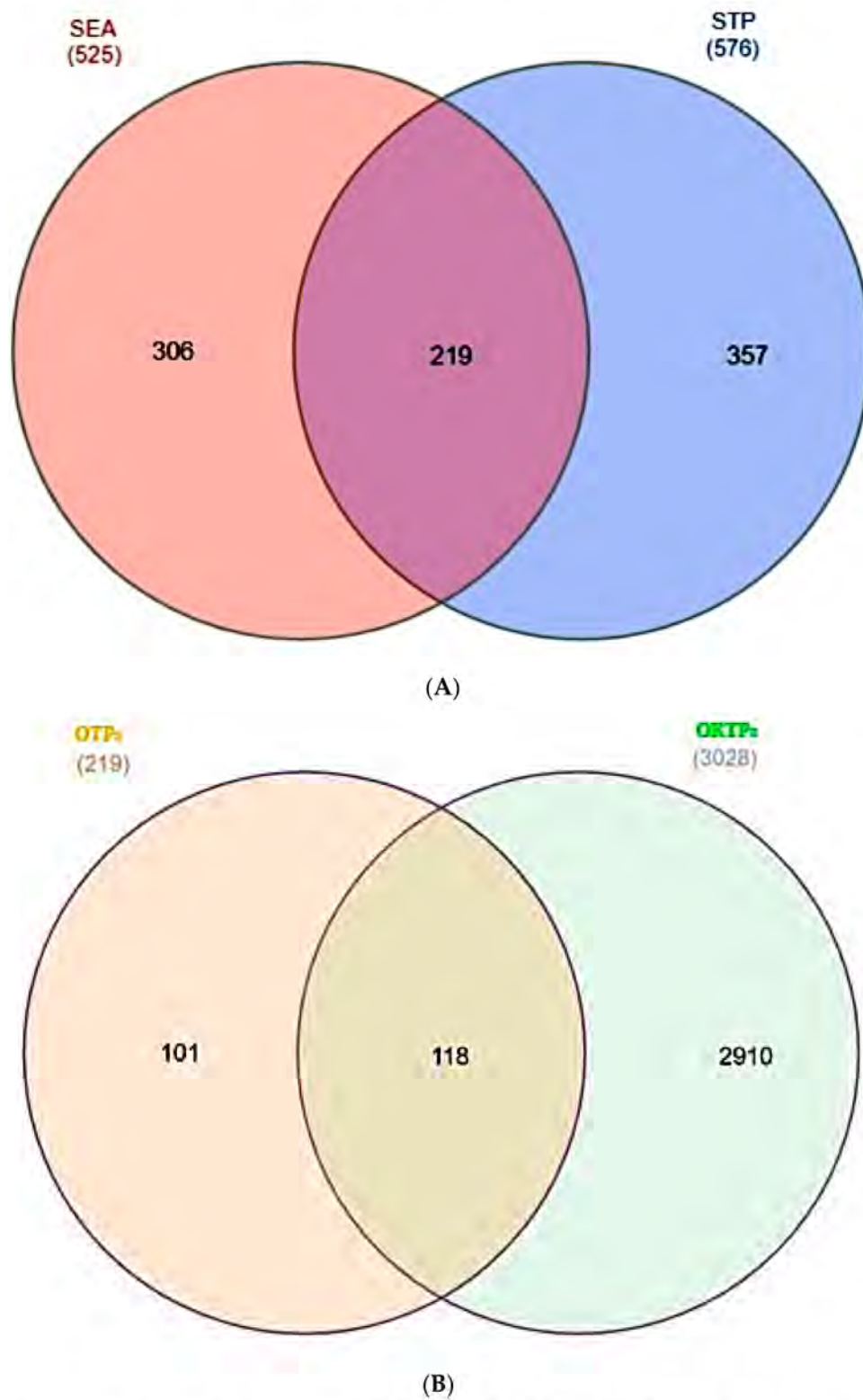
Figure 3. (**A**) The overlapping targets (219) between SEA and STP databases. (**B**) The final targets (118) between the overlapping target proteins (OTPs) (219) and obesity-related target proteins (ORTPs) (3028).

2.3. Overlapping Target Proteins between Obesity-Related Target Proteins and 219 Target Proteins

A total of 3028 target proteins associated with obesity were selected by retrieval from DisGeNET and OMIM databases (Supplementary Table S2). The Venn diagram result revealed 118 overlapping target proteins between obesity-associated 3028 target proteins and the 219 overlapping target proteins (Figure 3B) (Supplementary Table S3).

2.4. PPI Networks

From STRING analysis, the final overlapping 118 target proteins were directly related to obesity occurrence and progression, indicating 116 nodes and 674 edges (Figure 4). Two (PAM and RGS4) out of 118 targets did not interact with any other targets. In PPI networks, IL6 manifested the highest degree (52), followed by VEGFA (47), PTGS2 (42), MAPK1 (36), and CASP3 (36) (Table 3). Hence, IL6 was considered the uppermost target protein in PPI networks.
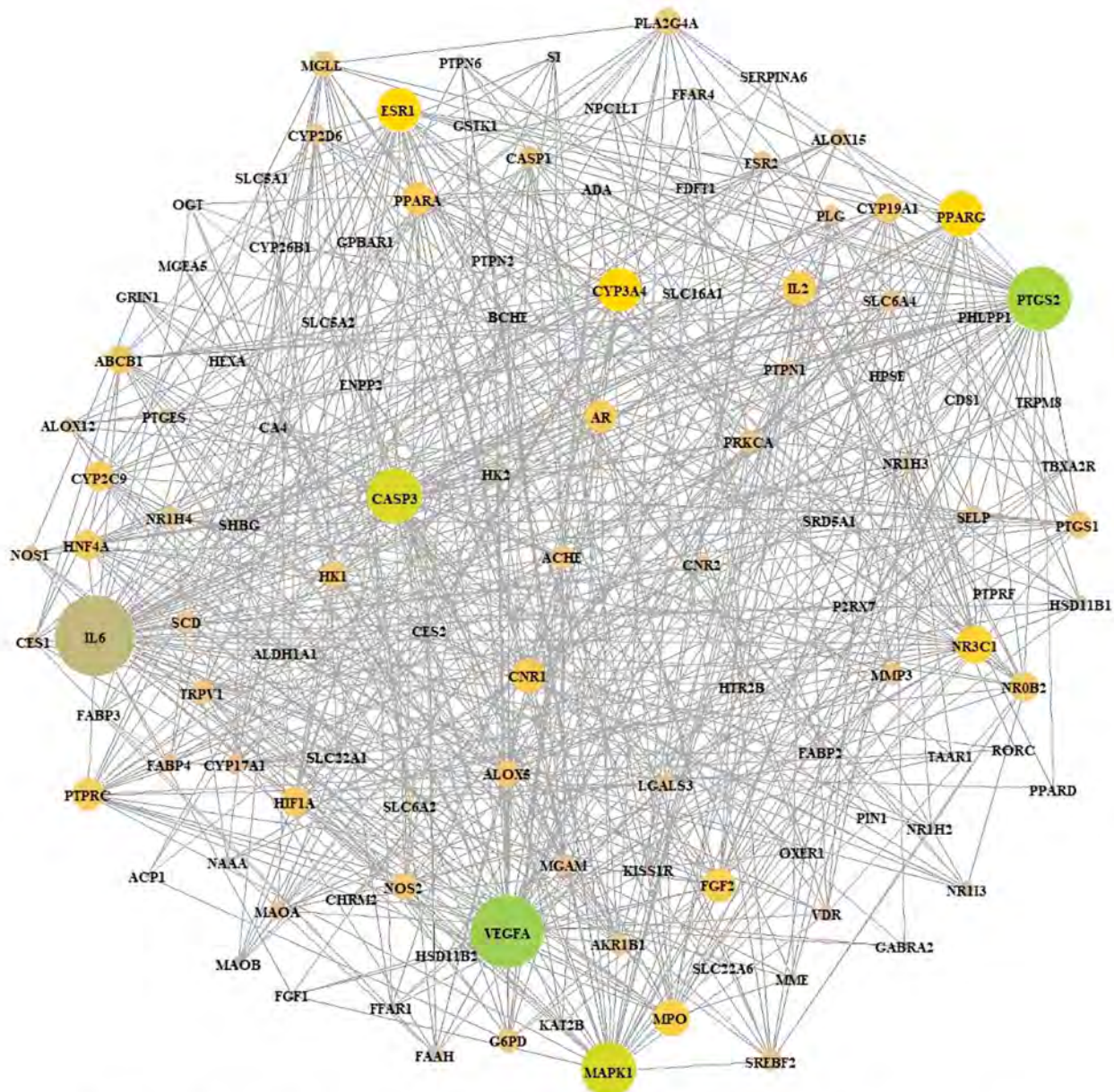

Figure 4. PPI networks (116 nodes and 674 edges). The size of circles stands for the degree of values.

Table 3. The degree value of 116 targets.

No.	Gene Symbol	Degree	No.	Gene Symbol	Degree
1	IL6	52	59	CES1	9
2	VEGFA	47	60	FABP2	9
3	PTGS2	42	61	HK2	9
4	CASP3	36	62	HSD11B1	9
5	MAPK1	36	63	NR1I3	9
6	PPARG	30	64	ADA	8
7	CYP3A4	29	65	ALDH1A1	8
8	ESR1	29	66	HTR2B	8
9	NR3C1	25	67	MAOB	8
10	MPO	23	68	PTPN6	8
11	CNR1	21	69	SLC6A2	8
12	FGF2	21	70	TBXA2R	8
13	IL2	21	71	BCHE	7
14	AR	20	72	FFAR4	7
15	PPARA	20	73	GPBAR1	7
16	PTPRC	20	74	KISS1R	7
17	CYP2C9	19	75	MGEA5	7
18	HIF1A	19	76	SI	7
19	HNF4A	19	77	SLC5A1	7
20	NR0B2	19	78	CES2	6
21	ABCB1	18	79	FABP3	6
22	CYP19A1	18	80	FFAR1	6
23	ALOX5	16	81	GRIN1	6
24	HK1	16	82	MME	6
25	MGLL	16	83	NAAA	6
26	NOS2	16	84	NR1H2	6
27	PLA2G4A	16	85	OGT	6
28	PTGS1	16	86	SRD5A1	6
29	ACHE	15	87	CHRM2	5
30	TRPV1	15	88	FGF1	5
31	G6PD	15	89	KAT2B	5
32	CASP1	14	90	NPC1L1	5
33	MMP3	14	91	PTPN2	5

Table 3. *Cont.*

No.	Gene Symbol	Degree	No.	Gene Symbol	Degree
34	PRKCA	14	92	SLC22A1	5
35	SREBF2	14	93	ACP1	4
36	AKR1B1	13	94	CD81	4
37	CYP2D6	13	95	CYP26B1	4
38	NR1H4	13	96	ENPP2	4
39	SCD	13	97	GABRA2	4
40	SLC6A4	13	98	P2RX7	4
41	CYP17A1	12	99	SLC16A1	4
42	ESR2	12	100	OXER1	4
43	MGAM	12	101	TAAR1	4
44	PLG	12	102	CA4	3
45	SELP	12	103	FDFT1	3
46	ALOX15	11	104	HSD11B2	3
47	CNR2	11	105	PPARD	3
48	FAAH	11	106	SERPINA6	3
49	FABP4	11	107	SLC5A2	3
50	LGALS3	11	108	PIN1	3
51	MAOA	11	109	TRPM8	3
52	NOS1	10	110	RORC	3
53	NR1H3	10	111	HPSE	2
54	PTGES	10	112	SLC22A6	2
55	PTPN1	10	113	PHLPP1	2
56	SHBG	10	114	PTPRF	2
57	VDR	10	115	GSTK1	1
58	ALOX12	9	116	HEXA	1

2.5. Analysis of Signaling Pathways against Obesity

The results of the KEGG (Kyoto Encyclopedia of Genes and Genomes) pathway enrichment analysis revealed that 22 signaling pathways were related to 42 target proteins (false discovery rate < 0.05). The 22 signaling pathways were directly connected to obesity, suggesting that these 22 signaling pathways might be the significant pathways of ICLs against obesity. The description of 22 signaling pathways is provided in Table 4. A bubble chart showed that both NOD-like receptor signaling pathway and MAPK signaling pathway have the same rich factor of 0.024 (Figure 5). Additionally, NOD-like receptor signaling pathway was directly related to IL6 (the highest degree of value) but MAPK signaling pathway was unconnected to IL6 (listed in Table 4).

Table 4. The number of 42 target proteins in 22 signaling pathways enrichment associated with obesity.

KEGG ID & Description	Target Proteins	False Discovery Rate
has03320:PPAR signaling pathway	PPARA,PPARG,FABP2,FABP3,FABP4,SCD,NR1H3	0.00000152
hsa04370:VEGF signaling pathway	PLA2G4A,PRKCA,PTGS2,VEGFA,MAPK1	0.00058
hsa04066:HIF-1 signaling pathway	PRKCA,VEGFA,MAPK1,IL6,NOS2,HIF1A,HK1,HK2	0.00000794
hsa04664:Fc epsilon RI signaling pathway	ALOX5,PLA2G4A,PRKCA,MAPK1	0.0047
hsa04917:Prolactin signaling pathway	MAPK1,ESR1,ESR2,CYP17A1	0.0051
hsa04657:IL-17 signaling pathway	MMP3,MAPK1,IL6,PTGS2,CASP3	0.0025
hsa04933:AGE-RAGE signaling pathway in diabetic complications	PRKCA,VEGFA,MAPK1,IL6,CASP3	0.0027
hsa04668:TNF signaling pathway	MMP3,MAPK1,IL6,PTGS2,CASP3	0.0037
hsa04020:Calcium signaling pathway	P2RX7,NOS1,NOS2,PRKCA,GRIN1,CHRM2,TBXA2R,HTR2B,PRKCA,MAPK1,HIF1A,ESR1,KAT2B	0.00028
hsa04919:Thyroid hormone signaling pathway	PRKCA,MAPK1,HIF1A,ESR1,KAT2B	0.0044
hsa04662:B cell receptor signaling pathway	MAPK1,PTPN6,CD81	0.0266
hsa04660:T cell receptor signaling pathway	PTPN6,PTPRC,IL2,MAPK1	0.0124
hsa04926:Relaxin signaling pathway	NOS1,PRKCA,VEGFA,MAPK1,NOS2	0.0062
hsa04910:Insulin signaling pathway	MAPK1,PTPRF,PTPN1,HK1,HK2	0.0066
hsa04015:Rap1 signaling pathway	FGF1,FGF2,VEGFA,MAPK1,PRKCA,GRIN1,CNR1	0.0024
hsa04912:GnRH signaling pathway	PLA2G4A,PRKCA,MAPK1	0.0411
hsa04014:RAS signaling pathway	FGF1,FGF2,PLA2G4A,VEGFA,MAPK1,PRKCA,GRIN1	0.0034
hsa04921:Oxytocin signaling pathway	PLA2G4A,PRKCA,PTGS2,MAPK1	0.0342
hsa04151:PI3K-Akt signaling pathway	FGF1,PHLPP1,FGF2,VEGFA,MAPK1,IL2,IL6,CHRM2,PRKCA	0.0025
hsa04630: Jak-STAT signaling pathway	PTPN2,PTPN6,IL2,IL6	0.0408
hsa04010:MAPK signaling pathway	FGF1,FGF2,PLA2G4A,VEGFA,PRKCA,MAPK1,CASP3	0.0093
hsa04621:NOD-like receptor signaling pathway	CASP1,P2RX7,MAPK1,IL6	0.0446
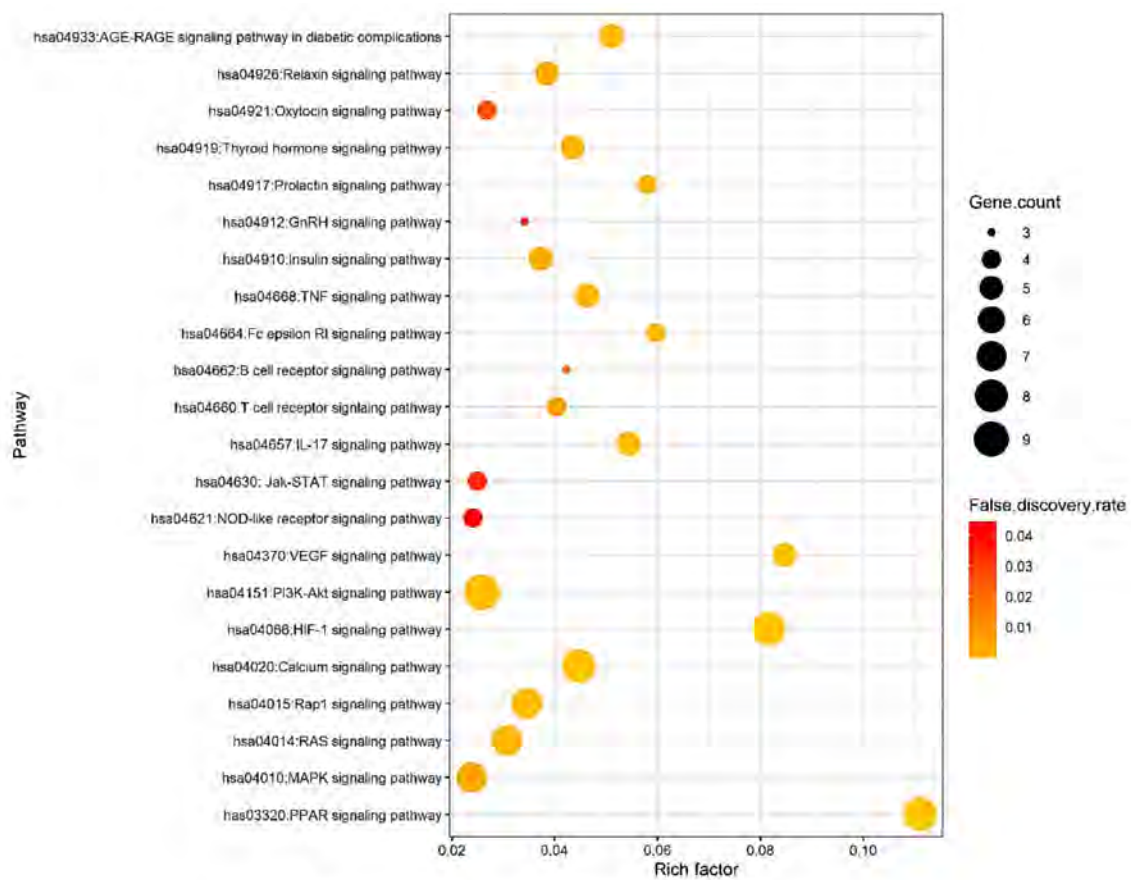
Figure 5. Bubble chart of ICLs against obesity.

2.6. STC Networks Analysis of ICLs against Obesity

STC networks of ICLs against obesity are exhibited in Figure 6. There were 22 pathways, 42 target proteins, and 39 compounds (103 nodes, 333 edges). The nodes stand for a total number of three components: signaling pathways—target proteins—compounds (STC). The edges stand for the association of a total number of three components. The STC networks suggested that the network was associated with the therapeutic efficacy against obesity. Particularly, MAPK1 target protein (the highest degree value) was related to 20 out of 22 signaling pathways in STC networks, connected to NOD-like receptor signaling pathway. The main three target proteins of ICLs against obesity are indicated in the KEGG pathway diagram (Figure 7).
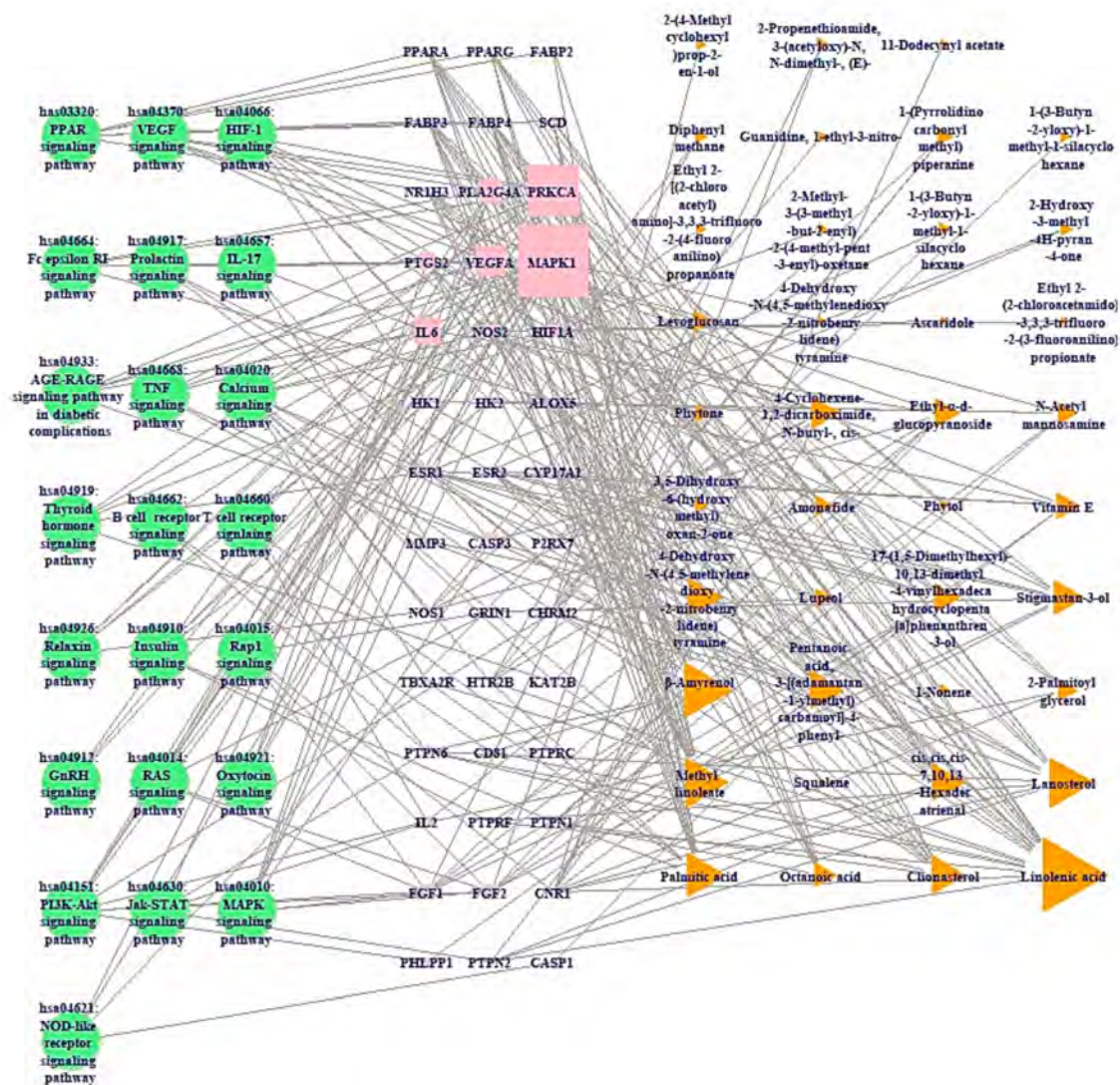
Figure 6. STC networks. Green circle: signaling pathway; pink square: target protein; orange triangle: compound.

KEGG pathway revealed location of the three target proteins (IL6, MAPK1, and CASP1) in intracellular components (Figure 7).
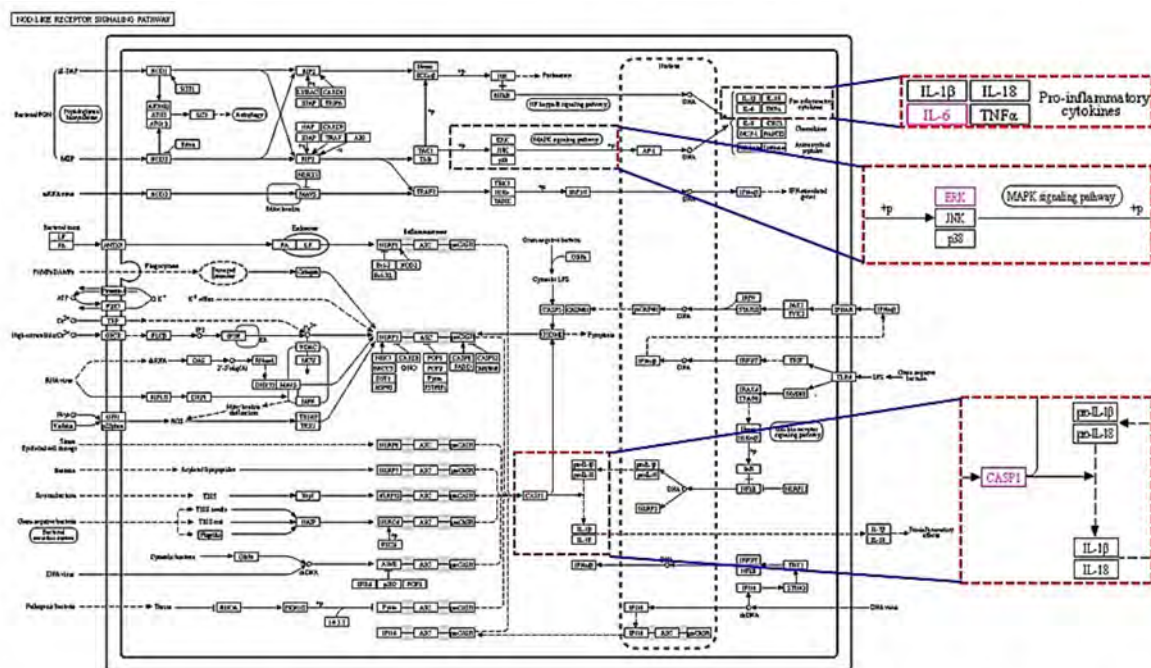
Figure 7. NOD-like receptor signaling pathway. Red dotted line indicated IL6; MAPK1 (known as ERK); and CASP1 location. Pink colors represent target proteins of ICLs on obesity.

2.7. KEGG Pathway Analysis of NLR Signaling Pathway

2.8. MDT of Four Target Proteins and 11 Compounds Connected to NLR Signaling Pathway

The IL6 protein (PDB ID: 4NI9) connected to three compounds on the NLR signaling pathway was used to perform MDT. It was observed that 3,5-dihydroxy-6-(hydroxymethyl)oxan-2-one) docked on the IL6 protein (PDB ID: 4NI9) exhibited the highest binding energy (−6.3 kcal/mol), followed by ethyl- α-d-glucopyranoside (−6.1 kcal/mol) and linolenic acid (−4.1 kcal/mol). The 3,5-dihydroxy-6-(hydroxymethyl)oxan-2-one also had the higher affinity than a positive control (veratric acid) [27] which showed −6.1 kcal/mol. The docking details of three compounds and a positive control are shown in Figure 8A, Table 5. The MDT of three compounds on MAPK1 (PDB ID: 4IZ5) was analyzed to identify the affinity. It was uncovered that 4-dehydroxy-N-(4,5-methylenedioxy-2-nitrobenzylidene)tyramine docked on an MAPK1 protein (PDB ID: 4IZ5) exposed the highest binding energy (−7.0 kcal/mol), followed by linolenic acid (-4.6 kcal/mol) and palmitic acid (−4.4 kcal/mol). Noticeably, 4-dehydroxy-N-(4,5-methylenedioxy-2-nitrobenzylidene) tyramine demonstrated higher affinity than a positive control (CU-Cpt 22) [28] showed −6.0 kcal/mol. The docking details of three compounds and a positive control are shown in Figure 8B, Table 6. The MDT score of four compounds on a P2RX7 protein (PDB ID: 5U2H) was analyzed to identify the affinity. It was exposed that pentanoic acid; 3-[(adamantan-1-ylmethyl)carbamoyl]-4-phenyl- docked on a P2RX7 protein (PDB ID: 5U2H) demonstrated the highest binding energy (−5.9 kcal/mol), followed by 4-cyclohexene-1,2-dicarboximide, N-butyl-, cis- (−4.1 kcal/mol), phytone (−3.3 kcal/mol), and cis,cis,cis-7,10,13-hexadecatrienal (−3.1 kcal/mol). The docking details of four compounds are shown in Table 7. Collectively, IL6 (PDB ID: 4NI9), MAPK1 (PDB ID:4IZ5), and P2RX7 (PDB ID: 5U2H) indicated that the affinity of each compound did not give a valid binding score (>−6.0 kcal/mol) [29]. Moreover, the affinity of four compounds on P2RX7 (PDB ID: 5U2H) was lower than the positive control (KN-62) [30] showed −9.8 kcal/mol.
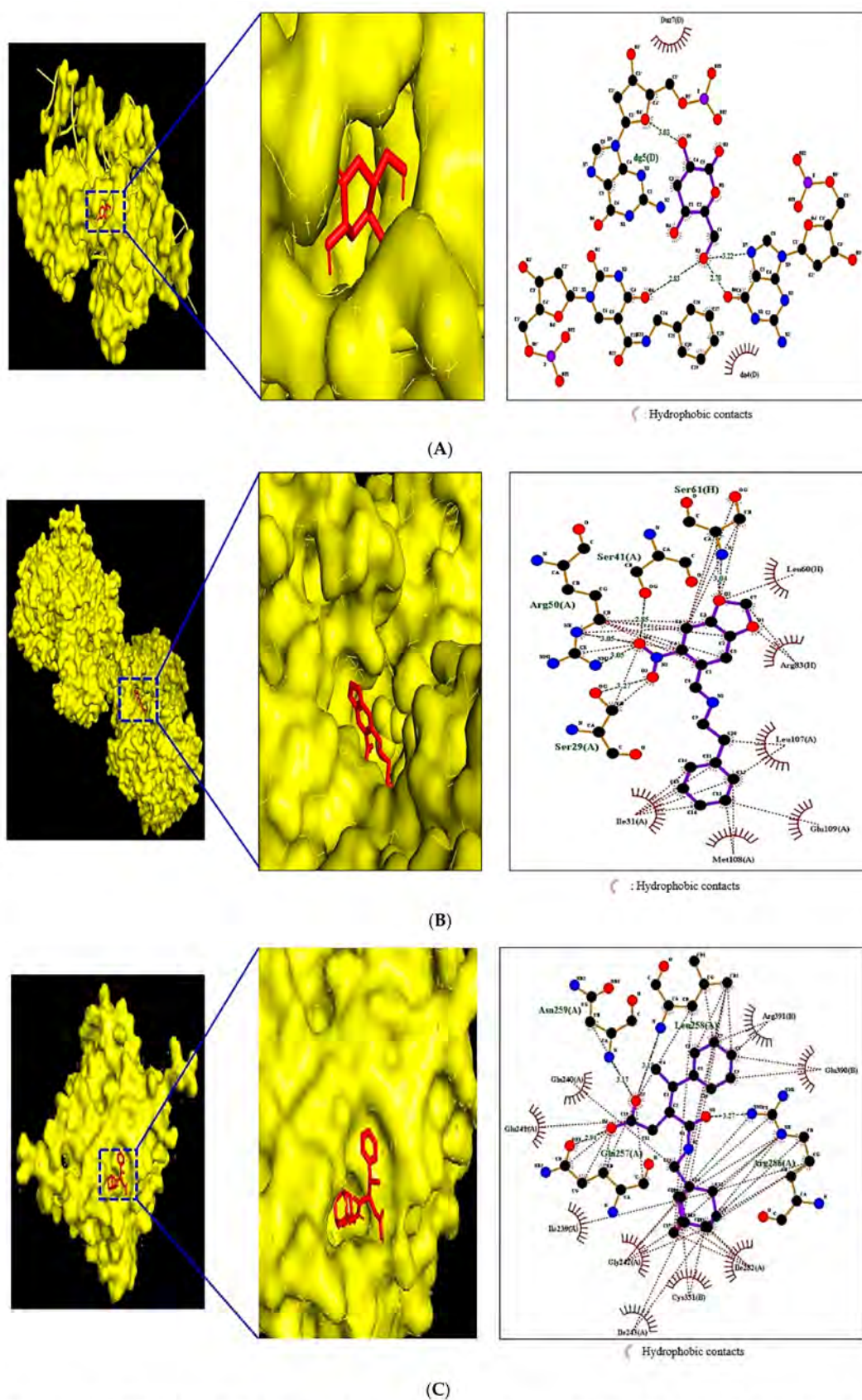
Figure 8. (**A**) MDT of three, 3,5-Dihydroxy-6-(hydroxymethyl) oxan-2-one on IL6 (PDB ID: 4NI9). (**B**) MDT of 4-dehydroxy-N-(4, 5-methylenedioxy- 2- nitrobenzylidene) tyramine on MAPK1 (PDB ID: 4IZ5). (**C**) MDT of pentanoic acid, 3-[(adamantan-1-ylmethyl) carbamoyl]-4-phenyl- on CASP1 (PDB ID: 3D6F).

Table 5. The binding energy of potential compounds and a positive control on IL6 (PDB ID: 4NI9).

Protein	Ligand	PubChem ID	Binding Energy (kcal/mol)	Hydrogen Bond Interactions Amino Acid Residue	Hydrophobic Interactions Amino Acid Residue
IL6 (PDB ID: 4NI9)	Linolenic acid	5,280,934	−4.1	N/A	Tyr31, Asp34, Gln111
	Ethyl-α-d-glucopyranoside	9,169,4274	−6.1	Arg16	Arg15
	3,5-Dihydroxy-6-(hydroxymethyl)oxan-2-one	541,561	−6.3	N/A	N/A

Protein	Positive control	PubChem ID	Binding energy(kcal/mol)	Hydrogen Bond Interactions Amino acid Residue	Hydrophobic Interactions Amino acid Residue
IL6 (PDB ID: 4NI9)	Veratric acid [27]	7121	−6.1	Arg16	N/A

Table 6. Binding energy of potential compounds and a positive control on MAPK1 (PDB ID: 4IZ5).

Protein	Ligand	PubChem ID	Binding Energy (kcal/mol)	Hydrogen Bond Interactions Amino Acid Residue	Hydrophobic Interactions Amino Acid Residue
MAPK1(PDB ID:4IZ5)	Palmitic acid	985	−4.4	Lys28, Ala26, Cys27 Met13, Glu186, Val14 Leu28, Arg15, Lys54 Glu12	Glu29, Asp30, Tyr62
	4-Dehydroxy-N-(4,5-methylenedioxy-2-nitrobenzylidene) tyramine	610,062	−7.0	Leu60, Arg83, Leu107	Ser61,Ser41,Arg50
	Linolenic acid	5,280,934	−4.6	Glu109, Met108, Ile31 Asn144	Ser29 Lys330, Glu303, Thr206 Lys207, Ser43, Ser47 Ser142, Leu8

Protein	Positive control	PubChem ID	Binding energy (kcal/mol)	Hydrogen Bond Interactions Amino acid Residue	Hydrophobic Interactions Amino acid Residue
MAPK1(PDB ID:4IZ5)	CU Cpt 22 [28]	71,503,400	−6.0	Thr12, Ile15	Thr41, Pro319, Lys138 Ile324, Asn13, Ser320 Gly42, Leu17, Leu20 Thr16

Table 7. Binding energy of potential compounds and a positive control on P2RX7 (PDB ID: 5U2H).

Protein	Ligand	PubChem ID	Binding Energy (kcal/mol)	Hydrogen Bond Interactions	Hydrophobic Interactions
				Amino Acid Residue	Amino Acid Residue
P2RX7(PDB ID: 5U2H)	Pentanoic acid, 3-[(adamantan-1-ylmethyl)carbamoyl]-4-phenyl-	4,920,612	−5.9	N/A	Val37, Phe344, Tyr343
					Val340, Tyr336, Leu45 Ile41, Tyr40
	Phytone	10,408	−3.3	N/A	Leu45, Tyr336, Ser339 Ile41, Val340, Tyr343 Val37, Ala44
	4-Cyclohexene-1,2-dicarboximide, N-butyl-, cis-	91,733,922	−4.1	N/A	Val37, Ile41, Tyr36
					Leu45, Ala44, Val340 Ser339, Tyr343
	cis,cis,cis-7,10,13-Hexadecatrienal	5,367,366	−3.1	N/A	Val340, Ile341, Gly345 Thr348, His34, Phe38 Phe344, Ile337
Protein	Positive control	PubChem ID	Binding energy(kcal/mol)	Hydrogen Bond Interactions	Hydrophobic Interactions
				Amino acid Residue	Amino acid Residue
P2RX7(PDB ID: 5U2H)	KN-62 [30]	5,312,126	−9.8	N/A	Tyr40, Ile41, Ala44
					Leu45, Tyr336, Val340 Tyr343, Ala347, Leu346

In addition, pentanoic acid; 3-[(adamantan-1-ylmethyl)carbamoyl]-4-phenyl-) docked on a CASP1 protein (PDB ID: 3D6F) showed a valid affinity (−7.3 kcal/mol), which was a comparatively higher affinity than three positive standard ligands (belnacasan [31], mulberroside A [32], and Q-VD-Oph [33]). The docking details of three compounds and the positive control are shown in Figure 8C, Table 8.

2.9. Toxicological Properties of Four Key Compounds

Additionally, toxicological properties of ethyl- α-d-glucopyranoside; 3,5-dihydroxy-6-(hydroxymethyl)oxan-2-one; 4-dehydroxy-N-(4,5-methylenedioxy-2-nitrobenzylidene)tyramine; and pentanoic acid, 3-[(adamantan-1-ylmethyl)carbamoyl]-4-phenyl- were predicted by ad-metSAR online tool. Our result suggested that the bioactives did not relate to Ames toxicity, carcinogenic properties, acute oral toxicity, and rat acute toxicity properties (Table 9).

Table 8. The binding energy of potential compounds and three positive controls on CASP1 (PDB ID: 3D6F).

Protein	Ligand	PubChem ID	Binding Energy (kcal/mol)	Hydrogen Bond Interactions Amino Acid Residue	Hydrophobic Interactions Amino Acid Residue
CASP1 (PDB ID: 3D6F)	Pentanoic acid, 3-[(adamantan-1-ylmethyl)carbamoyl]-4-phenyl-	4,920,612	−7.3	Asn259, Leu258, Arg286	Arg391, Glu390, Ile282
				Gln257	Cys331, Ile243, Gly242 Ile239, Glu241, Gln240

Protein	Positive Control	PubChem ID	Binding Energy (kcal/mol)	Hydrogen Bond Interactions Amino acid Residue	Hydrophobic Interactions Amino acid Residue
CASP1 (PDB ID: 3D6F)	Belnacasan [31]	11,398,092	−7.0	Arg286, Arg391	Cys285, Gly242, Ile239 Glu241, Gln240, Asn259 Leu258, Pro335, Ile282 Ala284, Ile243
	Mulberroside A [32]	6,443,484	−7.2	Val184, Asn132, Gln358 Asp381, Arg383	Gly188, Ile354, Met345 Arg352, Val348, Ile350 Gly351, Asp185
	Q-VD-Oph [33]	24,794,416	−7.2	Gln240, Leu258, Asn259	Cys285, Ile239, Arg286 Ile243, Gln257, Arg391 Glu390, Gly242, Ile282

Table 9. Toxicological properties of the highest affinity ligands on NOD-like receptor signaling pathway.

Parameters.	Compound Name			
	Ethyl-α-d-glucopyranoside	3,5-Dihydroxy-6-(hydroxymethyl)oxan-2-one	4-Dehydroxy-N-(4,5-methylenedioxy-2-nitrobenzylidene)tyramine	Pentanoic acid, 3-[(adamantan-1-ylmethyl)carbamoyl]-4-phenyl-
Ames toxicity	NAT	NAT	AT	NAT
Carcinogens	NC	NC	NC	NC
Acute oral toxicity	IV	III	III	III
Rat acute toxicity	0.9919	1.4924	2.6672	2.0497

AT: Ames toxic; NAT: Non Ames toxic; NC: Non-carcinogenic; Category-II means (50 mg/kg > LD50 < 500 mg/kg); Category-III means (500 mg/kg > LD50 < 5000 mg/kg); Category- IV means (LD50 > 5000 mg/kg).

3. Discussion

PPI networks indicated that IL6 was the uppermost target protein (based on the highest degree of value: 52 degrees) to treat obesity. Another STC network suggested that the therapeutic efficacy of ICLs on obesity was directly associated with 22 signaling pathways, 42 target proteins, and 39 compounds. The network exposed that mitogen-activated protein kinase 1 (MAPK1) (known as ERK) with the highest degree ranking (20 degrees), was the most significant target protein of ICLs against obesity. In this analysis,

the NLR signaling pathway was directly related to both IL6 and MAPK1, whereas the MAPK signaling pathway was not connected to IL6.

Thereby, the NLR signaling pathway was considered as a hub-signaling pathway of ICLs to ameliorate obesity; by constructing and analyzing the STC network, nine key compounds and four target proteins were obtained. The nine key compounds were linolenic acid (1); ethyl-α-d-glucopyranoside (2); 3,5-dihydroxy-6-(hydroxymethyl)oxan-2-one (3); palmitic acid (4); 4-dehydroxy-N-(4,5-methylenedioxy-2-nitrobenzylidene)tyramine (5); pentanoic acid, 3-[(adamantan-1-ylmethyl)carbamoyl]-4-phenyl- (6); phytone (7); 4-Cyclohexene-1,2-dicarboximide, N-butyl-cis- (8); cis,cis,cis-7,10,13-Hexadecatrienal (9). The four target proteins were IL6, MAPK1, P2RX7, and CASP1. MDT was performed between the 11 key compounds and four target proteins to verify network pharmacology results; where the value of MDT was compared with positive controls on each target protein. On MDT, the most potent compounds on IL6 were ethyl-α-d-glucopyranoside and 3,5-dihydroxy-6-(hydroxymethyl)oxan-2-one having an aliphatic heteromonocyclic structure. It was reported that a hetero-aliphatic ring is associated with a better appeal to develop a drug due to its high solubility, low lipophilicity (logP < 5), low albumin-binding and cytochrome P450 inhibition [34,35]. Similarly, Orlistat is a representative anti-obesity drug with an aliphatic heteromonocyclic structure [36] which implies that compounds with an aliphatic heteromonocyclic structure might be potential candidates for anti-obesity drug development.

On the MAPK1 target protein, the most potent compound was 4-dehydroxy-N-(4,5-methylenedioxy-2-nitrobenzylidene)tyramine with an aromatic heteropolycyclic structure. Likewise, Cetilistat is a typical drug for anti-obesity with an aromatic heteropolycyclic structure [36]. On the CASP1 target protein, the most potent compound was pentanoic acid, 3-[(adamantan-1-ylmethyl) carbamoyl] -4-phenyl-) with an aromatic homopolycyclic structure. Moreover, Oleoyl-estrone is a standard drug to reduce the body fat, having an aromatic homopolycyclic structure [36]. Based on these similarities, our study suggests that the four compounds in ICLs have a high chance of offering synergistic effects against obesity.

A bubble chart displayed that ICLs compounds on obesity were involved in 42 target proteins. Furthermore, the outputs of the KEGG pathway enrichment analysis of 42 target proteins indicated that 22 signaling pathways were connected to the progression of obesity, suggesting that these signaling pathways might be the molecular mechanisms of ICLs against obesity. The associations of the 22 signaling pathways with obesity were discussed as follows.

PPAR (peroxisome proliferator-activated receptor) signaling pathway: PPARs are ligand-regulated receptors, and many standard anti-obesity drugs are related to this signaling pathway [37]. VEGF (vascular endothelial growth factor) signaling pathway: VEGF-A (vascular endothelial growth factor A) has anti-inflammatory effects against diet-induced obesity [38]. HIF-1 (hypoxia-inducible factor 1) signaling pathway: inactivation of HIF-1 in adipose tissue alleviates obesity, suggesting that HIF-1 is a new target to develop anti-obesity agents [39]. Fc epsilon RI signaling pathway: an animal experiment demonstrated that mice with obesity increased the expression level of Fc epsilon RI more than eight times as compared to lean mice [40]. It implies that the inactivation of Fc epsilon RI can inhibit obesity. Prolactin signaling pathway: a report shows that prolactin accelerates fat accumulation in diverse animal models; particularly, an increased level of PRL was recorded for obese women in accordance with the visceral fat amount [41]. Interleukin 17 (IL17) signaling pathway: IL17 expression level is enhanced in obese individuals, a mediator to induce pro-inflammatory reactions [42,43]. AGE-RAGE signaling pathway in diabetic complications: AGE-RAGE is deeply interconnected to obesity-involved renal damage; both AGE and RAGE induce a pro-inflammatory reaction and are associated with obesity [44,45]. Tumor necrosis factor (TNF) signaling pathway: TNF inhibits lipoprotein lipase to break triglyceride, known as a primary factor of obesity [46]. Calcium signaling pathway: the activation of calcium signaling promotes energy consumption, which facili-

tates metabolism and differentiation of adipocytes, thus preventing obesity [47]. Thyroid signaling pathway: obesity is evidently related to Hashimoto's thyroiditis, suggesting that prevention of obesity is significant for recovering thyroid function [48]. B cell receptor signaling pathway: B cells aggravate obesity-related metabolic disorders and secrete cytokines to stimulate inflammation [49]. T cell receptor signaling pathway: T cell damage is accelerated by obesity; accordingly, T cell dysfunction is detrimental to maintain the immune system [50,51]. Relaxin signaling pathway: the activation of Relaxin-2 attenuates obesity in high-fat-diet mice; furthermore, Relaxin-3 associated with hypercholesterolemia is a potential target protein against obesity [52,53]. Insulin signaling pathway: insulin resistance is a crucial factor in aggravating obesity; especially, adipose tissues in obese individuals produce pro-inflammatory agents that stimulate progressive insulin resistance [54]. Rap-1 signaling pathway: an animal experiment demonstrated that the lack of Rap-1 induces weight gain due to abdominal fat accumulation [55]. Gonadotropin-releasing hormone (GnRH) signaling pathway: GnRH agonist treatment induces fat accumulation; mainly, inhibition of GnRH is a preventive method to treat obesity [56]. Renin-angiotensin system (RAS) signaling pathway: obesity is linked to RAS activation; in contrast, blockers of RAS diminished the type 2 diabetes by 22% in severe populations [57]. Oxytocin signaling pathway: the insufficiency of oxytocin and/or its receptor expression leads to obesity, which is implicated in metabolic disorders [58]. Phosphoinositide 3-Kinase—Protein kinase B (PI3K-AKT) signaling pathway: the dysfunction of the PI3K-AKT signaling pathway causes obesity, in other words, inhibition of the PI3K-AKT signaling pathway exacerbates metabolic processes [59]. Janus kinase/signal transducer and activator of transcription proteins (JAK-STAT) signaling pathway: the JAK-STAT signaling pathway is involved in preventing metabolic diseases including obesity, suggesting that the JAK-STAT pathway is a potential therapeutic mechanism for the treatment of obesity [60]. MAPK signaling pathway: a study indicated that obese mice have shown activated MAPK (known as ERK) expression, while the blocking of MAPK diminishes lipolysis in both mice and human adipose tissue [61]. NOD-like receptor (NLR) signaling pathway: the NLR pathway is overexpressed in the adipocytes from the obesity which increases inflammasome activity [62]. On NOD-like signaling pathway in KEGG pathway enrichment, each CASP1, MAPK1, and IL6 target protein is associated with proinflammatory reactions. In detail, CASP1, MAPK1, and IL6 are deeply involved in metabolic diseases, and their activation leads to obesity-related diseases [63].

According to the degree value of each target protein in the PPI network, IL6 was regarded as a key target of ICLs against obesity, which was directly connected to 52 out of 118 target proteins. In addition, based on the degree value of each target protein in the STC network, MAPK1 was considered as an uppermost target of ICLs against obesity, which was enriched in 20 out of 22 signaling pathways. Specifically, both the MAPK signaling pathway and the NLR signaling pathway had the same rich factor of 0.024. Between the two signaling pathways, a signaling pathway associated with IL6 and MAPK1 was the NLR signaling pathway. Thus, the NLR signaling pathway might be the key signaling pathway of ICLs against obesity. The four target proteins associated with the NLR signaling pathway were IL6, MAPK1, P2RX7, and MAPK1. The four target proteins were used to perform MDT with ligands connected to each target protein; also, MDT was conducted for positive controls to compare each affinity with ligands from ICLs. From the MDT, P2RX7 was excluded due to invalid binding energy (< -6.0 kcal/mol). Each ligand from ICLs bound to three other target proteins (IL6, MAPK1, and CASP1) and exposed higher affinity than the positive controls. Thus, these results suggest that inhibition of the three targets on the NLR signaling pathway might develop a synergistic effect to alleviate the obesity. Our research shows that four compounds, including ethyl-α-d-glucopyranoside (1); 3,5-dihydroxy-6-(hydroxymethyl)oxan-2-one (2); 4-dehydroxy-N-(4,5-methylenedioxy-2-nitrobenzylidenetyramine (3); and pentanoic acid, 3-[(adamantan-1-ylmethyl) carbamoyl] -4-phenyl- (4) from ICLs were noted as promising ligands on the three targets (IL6, MAPK1,and CASP1) (Figure 9).
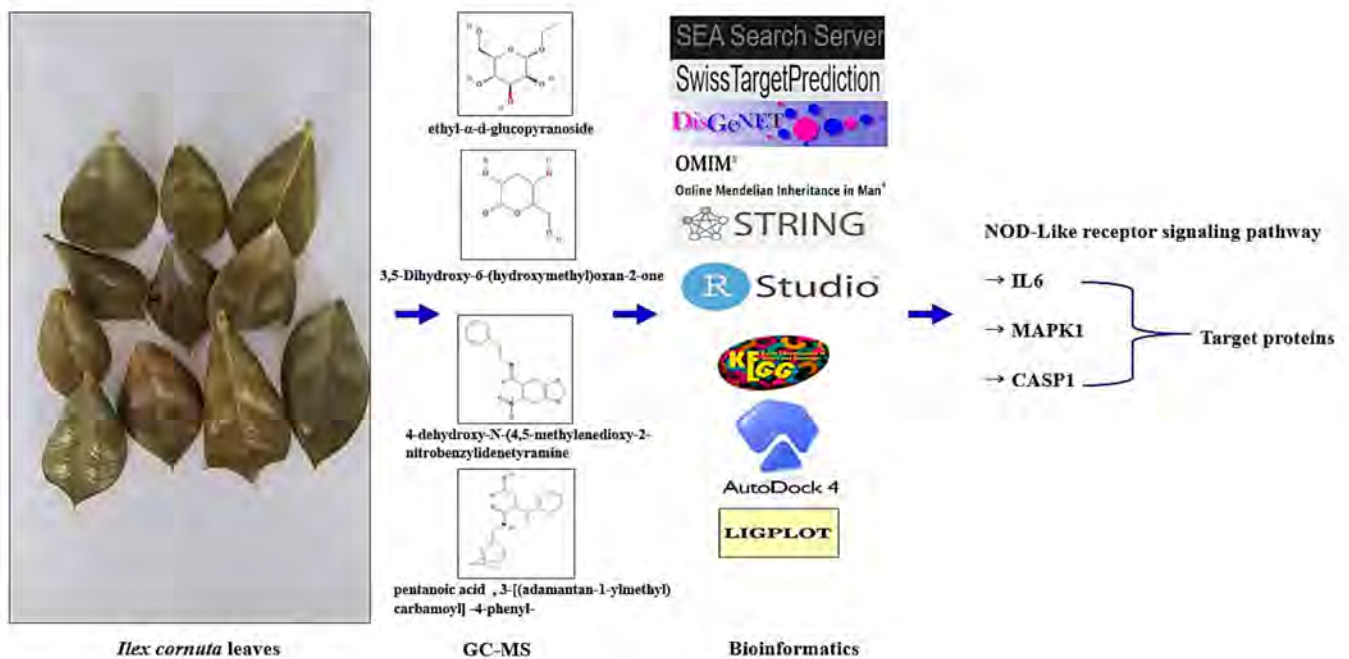
Figure 9. Summary figure of key findings in the study.

4. Materials and Methods

4.1. Plant Material Collection and Classification

The *Ilex cornuta* leaves (ICLs) were collected from Mihogil of Bomunmyeon (Latitude: 35.4023, Longitude: 126.3215), Jeollabuk-do, Republic of Korea, in October 2020, and the plant was identified by Dr. Dong Ha Cho, Plant Biologist and Professor at the Department of Bio-Health Convergence, College of Biomedical Science, Kangwon National University. A voucher number (KNL 011) was deposited at the Kenaf Corporation in the Department of Bio-Health Convergence, and the material can only be used for research purposes.

4.2. Plant Preparation and Extraction

The ICLs were dried in a shady area at room temperature (20–22 °C) for 7 days, and dried leaves were powdered using an electric blender. Approximately 30 g of *C. maackii* flower powder was soaked in 500 mL of 100% methanol (Daejung, Korea) for 7 days and repeated 3 times for the highest extraction. The solvent extract was collected, filtered, and evaporated using a vacuum evaporator (IKA- RV8, Japan). The evaporated sample was dried under a boiling water bath (IKA-HB10, Japan) at 40 °C to obtain the yield.

4.3. GC-MS Analysis Condition

Agilent 7890A was used to carry out the GC-MS analysis. The GC was equipped with a DB-5 (30 m × 0.25 mm × 0.25 μm) capillary column. Initially, the instrument was maintained at a temperature of 100 °C for 2.1 min. The temperature was increased to 300 °C at the rate of 25 °C/min and maintained for 20 min. The injection port temperature and helium flow rate were confirmed as 250 °C and 1.5 mL/min, respectively. The ionization voltage was 70 eV. The samples were injected in split mode at 10:1. The MS scan range was set at 35–900 (m/z). The fragmentation patterns of mass spectra were compared with those stored in the W8N05ST Library MS database. The percentage of each compound was calculated from the relative peak area of each compound in the chromatogram. The concept of integration used was the ChemStation integrated algorithms.

4.4. Chemical Compounds Database Construction and Drug-Likeness Identification

The chemical compounds from the ICLs leaves were identified through the GC-MS analysis. Then, the GC-MS detected chemical compounds that were filtered by Lipinski's

rule and TPSA value in SwissADME (http://www.swissadme.ch/) (accessed on 23 April 2021) [64] to confirm the 'drug-likeness' physicochemical properties. The PubChem repository (https://pubchem.ncbi.nlm.nih.gov/) (accessed on 23 April 2021) was utilized to select the SMILES (simplified molecular input line entry system) format.

4.5. Acquisition of Target Proteins Related to Selected Chemical Compounds or Obesity

Target proteins connected to the bioactives (using SMILES) were selected through both similarity ensemble approach (SEA) (http://sea.bkslab.org/)(accessed on 2 May 2021) [65] and SwissTargetPrediction (STP) (http://www.swisstargetprediction.ch/) (accessed on 2 May 2021) [20] with the '*Homo Sapiens*' setting. The obesity-related target proteins on humans were obtained from TTD (http://db.idrblab.net/ttd/) (accessed on 6 May 2021) and OMIM (https://www.omim.org/) (accessed on 6 May 2021). The overlapping target proteins between chemical compounds of ICLs and obesity-related target proteins were illustrated by InteractiVenn (http://www.interactivenn.net/) (accessed on 8 May 2021) [66].

4.6. PPI Networks and Signaling Pathways on a Bubble Chart

On the final overlapping target proteins, STRING (https://string-db.org/) (accessed on 11 May 2021) [67] was utilized to analyze the PPI networks. Thereby, RPackage was used to identify the degree of value, which is defined as the numbers of connectivity to a target protein (node). Then, signaling pathways directly related to obesity were visualized on a bubble chart via RPackage. Thus, the signaling pathways provide important clues for the therapeutic effect of ICLs against obesity.

4.7. A Signaling Pathways-Target Proteins-Chemical Compounds Network

The signaling pathways-target proteins-chemical compounds (STC) network was utilized to construct a size map, based on the degree of values. In the network, green circles (nodes) represented signaling pathways; pink rectangles (nodes) represented target proteins, and orange triangles (nodes) represented chemical compounds. The size of the pink rectangles stood for the number of connectivity with signaling pathways; the size of the orange triangles stood for the number of connectivity with target proteins. The merged networks were constructed using RPackage.

4.8. Preparation of Target Proteins for MDT

The target proteins of two key signaling pathways (MAPK signaling pathway, NOD-like receptor signaling pathway), i.e., FGF1 (PDB ID: 3OJ2), FGF2 (PDB ID: 1IIL), PLA2G4A (PDB ID: 1BCI), VEGFA (PDB ID: 3V2A), PRKCA (PDB ID: 3IW4), CASP3 (PDB ID: 5I9B), IL6 (PDB ID: 4NI9), MAPK1 (PDB ID: 4IZ5), P2RX7 (PDB ID: 5U2H), and CASP1 (PDB ID: 3D6F) were selected on STRING via RCSB PDB (https://www.rcsb.org/) (accessed on 12 May 2021). Thus, the target proteins selected as .pdb format were converted into .pdbqt format via Autodock (http://autodock.scripps.edu/) (accessed on 12 May 2021).

4.9. Preparation of Ligands for MDT

The ligand molecules were converted to .sdf from PubChem into .pdb format using Pymol, and the ligand molecules were converted into .pdbqt format through Autodock.

4.10. Preparation of Positive Standard Ligands on the NLR Signaling Pathway for MDT

The number of two positive standard ligands on IL6 (PDB ID: 4NI9) antagonists, i.e., veratric acid (PubChem ID: 7121); the number of one positive ligand on MAPK1 antagonist (PDB ID: 4IZ5), i.e., CU-Cpt 22 (PubChem ID: 71503400); the number of one positive ligand on P2RX7 (PDB ID: 5U2H), i.e., KN-62 (PubChem ID: 5312126); the number of three positive ligands on CASP1 (PDB ID: 3D6F), i.e., belnacasan (PubChem ID: 11398092), mulberroside A (PubChem ID: 6443484), and Q-VD-Oph (PubChem ID: 24794416) were selected to perform MDT.

4.11. Preparation of Ligand Molecules for MDT

The ligand molecules were converted to .sdf from PubChem into .pdb format using Pymol, and the ligand molecules were converted into .pdbqt format through Autodock.

4.12. Ligand-Protein Docking

The ligand molecules were docked with target proteins utilizing autodock4 by setting-up 4 energy range and 8 exhaustiveness as default to obtain 10 different poses of ligand molecules [68]. The active site's grid box size was $x = 40$ Å, $y = 40$Å, and $z = 40$Å. The 2D binding interactions were used with LigPlot+ v.2.2 (https://www.ebi.ac.uk/thornton-srv/software/LigPlus/) (accessed on 14 May 2021) [69]. After docking, ligands of the lowest binding energy (highest affinity) were selected to visualize the ligand-protein interaction in Pymol.

4.13. Toxicological Properties Prediction by admetSAR

Toxicological properties of key ligands from ICLs were demonstrated utilizing the admetSAR web-service tool (http://lmmd.ecust.edu.cn/admetsar1/predict/) (accessed on 14 May 2021) [70] because toxicity is a critical factor in developing new drugs. Hence, Ames toxicity, carcinogenic properties, acute oral toxicity, and rat acute toxicity were predicted by admetSAR.

5. Conclusions

In conclusion, we firstly analyzed the 'multi-signaling pathways—multi-target proteins—multi-compounds' network of ICLs against obesity via MDT. As a result, we found a key signaling pathway (NLR signaling pathway), three target proteins (IL6, MAPK1, and CASP1), and four compounds (ethyl-α-d-glucopyranoside; 3, 5-dihydroxy-6-(hydroxymethyl)oxan-2-one; 4-dehydroxy-N-(4,5-methylenedioxy-2 nitrobenzylidene) tyramine; and pentanoic acid, 3-[(adamantan-1-ylmethyl)carbamoyl]-4-phenyl-). Furthermore, the potential four compounds from ICLs have better affinity on each target protein than positive controls, suggesting that the compounds might be a new agent against obesity. Therefore, our research approach would be valuable for facilitating studies of herbal plants against obesity through network pharmacology.

Abbreviation

GnRH	Gonadotropin- Releasing Hormone
ICLs	*Ilex cornuta* leaves
IL17	Interleukin 17
Janus Kinase	Signal Transducer and Activator of Transcription proteins: JAK-STAT
MAPK1	Mitogen-activated protein kinase 1
MDT	Molecular Docking Test
NLR	NOD-like receptor
OTPs	Overlapping Target Proteins
ORTPs	Obesity-Related Target Proteins
PhosphoInositide	3-Kinase—Protein kinase B: PI3K-AKT
PPI	Protein–Protein Interaction
RAP1	Ras-proximate-1
SEA	Similarity Ensemble Approach
SMILES	Simplified Molecular Input Line Entry System
STC	Signaling pathways -Target proteins-Compounds
STP	SwissTargetPrediction
TNF	Tumor Necrosis Factor

References

1. Hurt, R.T.; Kulisek, C.; Buchanan, L.A.; McClave, S.A. The obesity epidemic: Challenges, health initiatives, and implications for gastroenterologists. *Gastroenterol. Hepatol.* **2010**, *6*, 780–792.
2. Hryhorczuk, C.; Sharma, S.; Fulton, S.E. Metabolic disturbances connecting obesity and depression. *Front. Neurosci.* **2013**, *7*, 177. [CrossRef] [PubMed]
3. Oh, K.K.; Adnan, M.; Ju, I.; Cho, D.H. A network pharmacology study on main chemical compounds fromHibiscus cannabinusL. leaves. *RSC Adv.* **2021**, *11*, 11062–11082. [CrossRef]
4. Artham, S.M.; Lavie, C.J.; Milani, R.V.; Ventura, H.O. Obesity and hypertension, heart failure, and coronary heart disease—Risk factor, paradox, and recommendations for weight loss. *Ochsner J.* **2009**, *9*, 124–132.
5. Shi, J.; Fan, J.; Su, Q.; Yang, Z. Cytokines and Abnormal Glucose and Lipid Metabolism. *Front. Endocrinol.* **2019**, *10*, 703. [CrossRef]
6. Rodgers, R.J.; Tschöp, M.H.; Wilding, J.P.H. Anti-obesity drugs: Past, present and future. *DMM Dis. Models Mech.* **2012**, *5*, 621–626. [CrossRef]
7. Kang, J.G.; Park, C.Y. Anti-obesity drugs: A review about their effects and safety. *Diabetes Metab. J.* **2012**, *36*, 13–25. [CrossRef]
8. Chy, M.N.U.; Adnan, M.; Chowdhury, M.R.; Pagano, E.; Kamal, A.T.M.M.; Oh, K.K.; Cho, D.H.; Capasso, R. Central and peripheral pain intervention by Ophiorrhiza rugosa leaves: Potential underlying mechanisms and insight into the role of pain modulators. *J. Ethnopharmacol.* **2021**, *276*, 114182.
9. Sun, N.N.; Wu, T.Y.; Chau, C.F. Natural dietary and herbal products in anti-obesity treatment. *Molecules* **2016**, *21*, 1351. [CrossRef]
10. KR101876617B1—Composition Comprising Extract of Ilex Cornuta for Promoting the Differentiation to Adipocytic Cells—Google Patents. Available online: https://patents.google.com/patent/KR101876617B1/en (accessed on 26 April 2021).
11. Kim, J.; Kang, W.; Min, H. In Vitro Anti-Inflammatory Activity of Ilex cornuta Extract Mediated by Inhibition of Extracellular Signal-Regulated Kinase Phosphorylation. *J. Med. Food* **2017**, *20*, 981–988. [CrossRef]
12. Ahn, E.M.; Asamenew, G.; Kim, H.W.; Lee, S.H.; Yoo, S.M.; Cho, S.M.; Cha, Y.S.; Kang, M.S. Anti-obesity effects of petasites japonicus (Meowi) ethanol extract on raw 264.7 macrophages and 3t3-l1 adipocytes and its characterization of polyphenolic compounds. *Nutrients* **2020**, *12*, 1261. [CrossRef]
13. Hao, D.; Gu, X.; Xiao, P.; Liang, Z.; Xu, L.; Peng, Y. Research progress in the phytochemistry and biology of Ilex pharmaceutical resources. *Acta Pharm. Sin. B* **2013**, *3*, 8–19. [CrossRef]
14. Oh, K.K.; Adnan, M.; Cho, D.H. Network pharmacology approach to decipher signaling pathways associated with target proteins of NSAIDs against COVID-19. *Sci. Rep.* **2021**, *11*, 9606. [CrossRef]
15. Chandran, U.; Mehendale, N.; Patil, S.; Chaguturu, R.; Patwardhan, B. Network Pharmacology. In *Innovative Approaches in Drug Discovery: Ethnopharmacology, Systems Biology and Holistic Targeting*; Elsevier Inc.: Amsterdam, The Netherlands, 2017; pp. 127–164. ISBN 9780128018224.
16. Oh, K.K.; Adnan, M.; Cho, D.H. Network pharmacology of bioactives from Sorghum bicolor with targets related to diabetes mellitus. *PLoS ONE* **2020**, *15*, e0240873. [CrossRef]
17. Oh, K.K.; Adnan, M.; Cho, D.H. Active ingredients and mechanisms of Phellinus linteus (grown on Rosa multiflora) for alleviation of Type 2 diabetes mellitus through network pharmacology. *Gene* **2020**, *768*, 145320. [CrossRef]
18. Shen, L.; Chen, W.; Zhang, B.; Liu, L.; Cao, Y. Integrating network pharmacology and bioinformatics analysis to explore the mechanism of Yupingfengsan in treating lung adenocarcinoma. *Eur. J. Integr. Med.* **2019**, *31*, 100967. [CrossRef]
19. Wang, Z.; Liang, L.; Yin, Z.; Lin, J. Improving chemical similarity ensemble approach in target prediction. *J. Cheminformatics* **2016**, *8*, 20. [CrossRef]

20. Daina, A.; Michielin, O.; Zoete, V. SwissTargetPrediction: Updated data and new features for efficient prediction of protein targets of small molecules. *Nucleic Acids Res.* **2019**, *47*, W357–W3664. [CrossRef]

21. Piñero, J.; Queralt-Rosinach, N.; Bravo, À.; Deu-Pons, J.; Bauer-Mehren, A.; Baron, M.; Sanz, F.; Furlong, L.I. DisGeNET: A discovery platform for the dynamical exploration of human diseases and their genes. *Database* **2015**, *2015*, 1–17. [CrossRef]

22. Hamosh, A.; Scott, A.F.; Amberger, J.S.; Bocchini, C.A.; McKusick, V.A. Online Mendelian Inheritance in Man (OMIM), a knowledgebase of human genes and genetic disorders. *Nucleic Acids Res.* **2005**, *33*, D514. [CrossRef]

23. Zeng, X.; Zhang, P.; He, W.; Qin, C.; Chen, S.; Tao, L.; Wang, Y.; Tan, Y.; Gao, D.; Wang, B.; et al. NPASS: Natural product activity and species source database for natural product research, discovery and tool development. *Nucleic Acids Res.* **2018**, *46*, D1217–D1222. [CrossRef]

24. Hilgren, J.D.; Salverda, J.A. Antimicrobial Efficacy of a Peroxyacetic/Octanoic Acid Mixture in Fresh-Cut-Vegetable Process Waters. *J. Food Sci.* **2000**, *65*, 1376–1379. [CrossRef]

25. Saleem, M. Lupeol, a novel anti-inflammatory and anti-cancer dietary triterpene. *Cancer Lett.* **2009**, *285*, 109–115. [CrossRef]

26. Yuan, X.; Sun, H.; Liu, Y.; Shiroshita, T.; Kawano, S.; Takeshi, S.; Ma, J.; Zhang, Z. Anti-cancer activity comparisons of aqueous extracts from Inonotus obliquus, Cordyceps militaris and Uncaria tomentosa in vitro and in vivo. *J. Pharmacogn. Phytochem.* **2014**, *2*, 19–25.

27. Wang, Q.B.; Sun, L.Y.; Du, Y. Veratric Acid Inhibits LPS-Induced IL-6 and IL-8 Production in Human Gingival Fibroblasts. *Inflammation* **2016**, *39*, 237–242. [CrossRef]

28. Tamai, R.; Suzuki, K.; Mashima, I.; Kiyoura, Y. MPMBP down-regulates Toll-like receptor (TLR) 2 ligand-induced proinflammatory cytokine production by inhibiting NF-κB but not AP-1 activation. *Int. Immunopharmacol.* **2020**, *79*. [CrossRef]

29. Shityakov, S.; Förster, C. In silico predictive model to determine vector-mediated transport properties for the blood-brain barrier choline transporter. *Adv. Appl. Bioinform. Chem.* **2014**. [CrossRef]

30. Shen, L.; Yang, Q.; He, Y.; Zou, X.; Cao, Z. BmK NT1-induced neurotoxicity is mediated by PKC/CaMKII-dependent ERK1/2 and p38 activation in primary cultured cerebellar granule cells. *Toxicology* **2019**, *421*, 22–29. [CrossRef]

31. Xu, S.; Li, X.; Liu, Y.; Xia, Y.; Chang, R.; Zhang, C. Inflammasome inhibitors: Promising therapeutic approaches against cancer. *J. Hematol. Oncol.* **2019**, *12*, 1–13. [CrossRef]

32. Chan, K.-C.; Ho, H.-H.; Lin, M.-C.; Huang, C.-N.; Huang, H.-P.; Wang, C.-J. Impact of polyphenolic components from mulberry on apoptosis of vascular smooth muscle cells. *J. Sci. Food Agric.* **2016**, *96*, 381–391. [CrossRef]

33. Renolleau, S.; Fau, S.; Goyenvalle, C.; Joly, L.M.; Chauvier, D.; Jacotot, E.; Mariani, J.; Charriaut-Marlangue, C. Specific caspase inhibitor Q-VD-OPh prevents neonatal stroke in P7 rat: A role for gender. *J. Neurochem.* **2007**, *100*, 1062–1071. [CrossRef] [PubMed]

34. Aldeghi, M.; Malhotra, S.; Selwood, D.L.; Chan, A.W.E. Two- and three-dimensional rings in drugs. *Chem. Biol. Drug Des.* **2014**, *83*, 450–461. [CrossRef] [PubMed]

35. Chen, X.; Li, H.; Tian, L.; Li, Q.; Luo, J.; Zhang, Y. Analysis of the Physicochemical Properties of Acaricides Based on Lipinski's Rule of Five. *J. Comput. Biol.* **2020**, *27*, 1397–1406. [CrossRef] [PubMed]

36. Wishart, D.S.; Knox, C.; Guo, A.C.; Shrivastava, S.; Hassanali, M.; Stothard, P.; Chang, Z.; Woolsey, J. DrugBank: A comprehensive resource for in silico drug discovery and exploration. *Nucleic Acids Res.* **2006**, *34*. [CrossRef]

37. Blaschke, F.; Takata, Y.; Caglayan, E.; Law, R.E.; Hsueh, W.A. Obesity, peroxisome proliferator-activated receptor, and atherosclerosis in type 2 diabetes. *Arterioscler. Thromb. Vasc. Biol.* **2006**, *26*, 28–40. [CrossRef]

38. Elias, I.; Franckhauser, S.; Bosch, F. New insights into adipose tissue VEGF-A actions in the control of obesity and insulin resistance. *Adipocyte* **2013**, *2*, 109–112. [CrossRef]

39. Jiang, C.; Qu, A.; Matsubara, T.; Chanturiya, T.; Jou, W.; Gavrilova, O.; Shah, Y.M.; Gonzalez, F.J. Disruption of hypoxia-inducible factor 1 in adipocytes improves insulin sensitivity and decreases adiposity in high-fat diet-fed mice. *Diabetes* **2011**, *60*, 2484–2495. [CrossRef]

40. Nadler, S.T.; Stoehr, J.P.; Schueler, K.L.; Tanimoto, G.; Yandell, B.S.; Attie, A.D. The expression of adipogenic genes is decreased in obesity and diabetes mellitus. *Proc. Natl. Acad. Sci. USA* **2000**, *97*, 11371–11376. [CrossRef]

41. Kok, P.; Roelfsema, F.; Frölich, M.; Meinders, A.E.; Pijl, H. Prolactin Release Is Enhanced in Proportion to Excess Visceral Fat in Obese Women. *J. Clin. Endocrinol. Metab.* **2004**, *89*, 4445–4449. [CrossRef]

42. Ahmed, M.; Gaffen, S.L. IL-17 in obesity and adipogenesis. *Cytokine Growth Factor Rev.* **2010**, *21*, 449–453. [CrossRef]

43. Zúñiga, L.A.; Shen, W.-J.; Joyce-Shaikh, B.; Pyatnova, E.A.; Richards, A.G.; Thom, C.; Andrade, S.M.; Cua, D.J.; Kraemer, F.B.; Butcher, E.C. IL-17 Regulates Adipogenesis, Glucose Homeostasis, and Obesity. *J. Immunol.* **2010**, *185*, 6947–6959. [CrossRef]

44. Tomino, Y.; Hagiwara, S.; Gohda, T. AGE-RAGE interaction and oxidative stress in obesity-related renal dysfunction. *Kidney International* **2011**, *80*, 133–135. [CrossRef]

45. Leuner, B.; Max, M.; Thamm, K.; Kausler, C.; Yakobus, Y.; Bierhaus, A.; Sel, S.; Hofmann, B.; Silber, R.E.; Simm, A.; et al. RAGE beeinflusst adipositas bei mäusen. einfluss des rezeptors für AGEs (RAGE) auf gewichtszunahme, insulin-und AGE-akkumulation in mäusen unter hochfettdiät. *Zeitschrift für Gerontologie und Geriatrie* **2012**, *45*, 102–108. [CrossRef]

46. Kern, P.A.; Ranganathan, S.; Li, C.; Wood, L.; Ranganathan, G. Adipose tissue tumor necrosis factor and interleukin-6 expression in human obesity and insulin resistance. *Am. J. Physiol. Endocrinol. Metab.* **2001**, *280*, 745–751. [CrossRef]

47. Song, Z.; Wang, Y.; Zhang, F.; Yao, F.; Sun, C. Calcium signaling pathways: Key pathways in the regulation of obesity. *Int. J. Mol. Sci.* **2019**, *20*, 2768. [CrossRef]

48. Song, R.H.; Wang, B.; Yao, Q.M.; Li, Q.; Jia, X.; Zhang, J.A. The Impact of Obesity on Thyroid Autoimmunity and Dysfunction: A Systematic Review and Meta-Analysis. *Front. Immunol.* **2019**, *10*, 2349. [CrossRef]
49. Liu, R.; Nikolajczyk, B.S. Tissue immune cells fuel obesity-associated inflammation in adipose tissue and beyond. *Front. Immunol.* **2019**, *10*, 1587. [CrossRef]
50. Shirakawa, K.; Yan, X.; Shinmura, K.; Endo, J.; Kataoka, M.; Katsumata, Y.; Yamamoto, T.; Anzai, A.; Isobe, S.; Yoshida, N.; et al. Obesity accelerates T cell senescence in murine visceral adipose tissue. *J. Clin. Investig.* **2016**, *126*, 4626–4639. [CrossRef]
51. Aguilar, E.G.; Murphy, W.J. Obesity induced T cell dysfunction and implications for cancer immunotherapy. *Curr. Opin. Immunol.* **2018**, *51*, 181–186. [CrossRef]
52. Lee, K.C.; Hsieh, Y.C.; Chan, C.C.; Sun, H.J.; Huang, Y.H.; Hou, M.C.; Lin, H.C. Human relaxin-2 attenuates hepatic steatosis and fibrosis in mice with non-alcoholic fatty liver disease. *Lab. Investig.* **2019**, *99*, 1203–1216. [CrossRef]
53. Smith, C.M.; Walker, A.W.; Hosken, I.T.; Chua, B.E.; Zhang, C.; Haidar, M.; Gundlach, A.L. Relaxin-3/RXFP3 networks: An emerging target for the treatment of depression and other neuropsychiatric diseases? *Front. Pharmacol.* **2014**, *5*, 46. [CrossRef]
54. Kahn, S.E.; Hull, R.L.; Utzschneider, K.M. Mechanisms linking obesity to insulin resistance and type 2 diabetes. *Nature* **2006**, *444*, 840–846. [CrossRef]
55. Martínez, P.; Gómez-López, G.; García, F.; Mercken, E.; Mitchell, S.; Flores, J.M.; deCabo, R.; Blasco, M.A. RAP1 Protects from Obesity through Its Extratelomeric Role Regulating Gene Expression. *Cell Rep.* **2013**, *3*, 2059–2074. [CrossRef]
56. Yamasaki, H.; Douchi, T.; Yamamoto, S.; Toshimichi, O.; Kuwahata, R.; Nagata, Y. Body fat distribution and body composition during GnRH agonist therapy. *Obstet. Gynecol.* **2001**, *97*, 338–342. [CrossRef]
57. Goossens, G.H. The Renin-Angiotensin System in the Pathophysiology of Type 2 Diabetes. *Obes. Facts* **2012**, *5*, 611–624. [CrossRef]
58. Ding, C.; Leow, M.K.S.; Magkos, F. Oxytocin in metabolic homeostasis: Implications for obesity and diabetes management. *Obes. Rev.* **2019**, *20*, 22–40. [CrossRef]
59. Huang, X.; Liu, G.; Guo, J.; Su, Z.Q. The PI3K/AKT pathway in obesity and type 2 diabetes. *Int. J. Biol. Sci.* **2018**, *14*, 1483–1496. [CrossRef]
60. Dodington, D.W.; Desai, H.R.; Woo, M. JAK/STAT—Emerging Players in Metabolism. *Trends Endocrinol. Metab.* **2018**, *29*, 55–65. [CrossRef]
61. Hong, S.; Song, W.; Zushin, P.J.H.; Liu, B.; Jedrychowski, M.P.; Mina, A.I.; Deng, Z.; Cabarkapa, D.; Hall, J.A.; Palmer, C.J.; et al. Phosphorylation of Beta-3 adrenergic receptor at serine 247 by ERK MAP kinase drives lipolysis in obese adipocytes. *Mol. Metab.* **2018**, *12*, 25–38. [CrossRef] [PubMed]
62. Yin, Z.; Deng, T.; Peterson, L.E.; Yu, R.; Lin, J.; Hamilton, D.J.; Reardon, P.R.; Sherman, V.; Winnier, G.E.; Zhan, M.; et al. Transcriptome analysis of human adipocytes implicates the NOD-like receptor pathway in obesity-induced adipose inflammation. *Mol. Cell. Endocrinol.* **2014**, *394*, 80–87. [CrossRef]
63. Febbraio, M.A. Role of interleukins in obesity: Implications for metabolic disease. *Trends Endocrinol. Metab.* **2014**, *25*, 312–319. [CrossRef] [PubMed]
64. Daina, A.; Michielin, O.; Zoete, V. SwissADME: A free web tool to evaluate pharmacokinetics, drug-likeness and medicinal chemistry friendliness of small molecules. *Sci. Rep.* **2017**, *7*. [CrossRef] [PubMed]
65. Keiser, M.J.; Roth, B.L.; Armbruster, B.N.; Ernsberger, P.; Irwin, J.J.; Shoichet, B.K. Relating protein pharmacology by ligand chemistry. *Nat. Biotechnol.* **2007**, *25*, 197–206. [CrossRef]
66. Heberle, H.; Meirelles, V.G.; da Silva, F.R.; Telles, G.P.; Minghim, R. InteractiVenn: A web-based tool for the analysis of sets through Venn diagrams. *BMC Bioinform.* **2015**, *16*, 169. [CrossRef]
67. Szklarczyk, D.; Gable, A.L.; Lyon, D.; Junge, A.; Wyder, S.; Huerta-Cepas, J.; Simonovic, M.; Doncheva, N.T.; Morris, J.H.; Bork, P.; et al. STRING v11: Protein-protein association networks with increased coverage, supporting functional discovery in genome-wide experimental datasets. *Nucleic Acids Res.* **2019**, *47*, D607–D613. [CrossRef]
68. Khanal, P.; Patil, B.M.; Chand, J.; Naaz, Y. Anthraquinone Derivatives as an Immune Booster and their Therapeutic Option Against COVID-19. *Nat. Prod. Bioprospect.* **2020**, *10*, 325–335. [CrossRef]
69. Wallace, A.C.; Laskowski, R.A.; Thornton, J.M. Ligplot: A program to generate schematic diagrams of protein-ligand interactions. *Protein Eng. Des. Sel.* **1995**, *8*, 127–134. [CrossRef]
70. Yang, H.; Lou, C.; Sun, L.; Li, J.; Cai, Y.; Wang, Z.; Li, W.; Liu, G.; Tang, Y. admetSAR 2.0: Web-service for prediction and optimization of chemical ADMET properties. *Bioinformatics* **2019**, *35*, 1067–1069. [CrossRef]